Photon generation by injection of electrons via quantum Hall edge channels

Kenji Ikushima[1,2] and Susumu Komiyama[3]

[1]*Department of Applied Physics, Tokyo University of Agriculture and Technology, Nakacho, Koganei, Tokyo 184-8588, Japan*

[2]*PRESTO, Japan Science and Technology Agency, Kawaguchi, Saitama 332-0012, Japan*

[3]*Department of Basic Science, University of Tokyo, Komaba, Meguro, Tokyo 153-8902, Japan*

(Received 12 September 2011; published 17 October 2011)

Photon emission caused by quantum electron transport has been found in the quantum Hall effect regime through photon-counting THz microscopy. The imaging reveals that Landau-level emission occurs at the confluence of unequally occupied edge channels in the quantum Hall effect plateau (filling factor $\nu = 4$) when a potential barrier across the Hall bar is introduced. It is also found that the confluence at the lower-potential sample boundary (with positive Hall voltage) emits more photons than that at the higher-potential one. Since electrons and holes are injected via phase-coherent conducting channels, this photon emission phenomenon will provide a new platform for studying the interplay between quantum electron transport and quantum optics.

DOI: 10.1103/PhysRevB.84.155313 PACS number(s): 73.43.−f, 42.50.−p, 78.67.−n

I. INTRODUCTION

An electron flow emitted from an electron source can be noiseless because no two identical electrons may occupy the same quantum state simultaneously according to the Pauli exclusion principle. Electron antibunching has been successfully observed in electron currents constrained to flow in a two-dimensional mesoscopic semiconductor device, and results in the quantized conductance observed in quantum point contacts (QPC's) or precise quantization of Hall resistance in strong magnetic fields. In contrast, a photon flow emitted from a light source in thermal equilibrium exhibits super-Poissonian fluctuations, which originate from photon bunching due to bosonic stimulation.

Pioneering experiments on suppression of photon-number fluctuations were performed using commercial semiconductor light-emitting devices in the late 1980s.[1] Nonclassical photon generation below the Poisson limit was found by reducing current fluctuations with a high impedance external electron source. To transfer the fermionic statistics of electrons to photons, noiseless transport in quantum conductors would be an appealing approach to current injection for photon generation. Current fluctuation in QPC's is thus an important research topic.[2–6] It has been theoretically suggested that sub-Poissonian statistics inherited from electrons can be transferred to photons of gigahertz radiation emitted from a QPC.[2,3] Several experimental techniques have been developed to measure the high-frequency quantum shot noise of QPC's.[4–6]

The aim of the present work is to establish an alternative physical system for photon generation associated with quantum electron transport. A two-dimensional electron gas (2DEG) in a strong magnetic field is a powerful platform that offers the possibility of manipulating noiseless currents in solid-state devices.[7] In the quantum Hall effect (QHE) regime, edge channels serve as well-defined one-dimensional conducting channels, for which electrically controlled beam splitters can be used. Edge channels have been utilized in quantum interference demonstrations such as the fermionic Hanbury Brown–Twiss experiment[8] and an electronic Mach-Zehnder interferometer.[9] Since electrons are carried by edge channels without backscattering over a macroscopic length, photon generation by means of edge channels will provide a new opportunity to study the interplay between quantum electron transport and quantum optics. Although we reported terahertz (THz) emission with respect to edge channels in an earlier work,[10] the reported emission process arises from current injection through classical drift motion of electrons due to the Hall electric field in a dissipative bulk state. In this paper, we report THz-photon generation by injection of electrons via edge-channel transport.

Here, we introduce a potential barrier by negatively biasing a cross gate in a QHE device [Fig. 1(a)]. Edge channels are selectively populated according to the potential barrier when the filling factor beneath the gate, ν_G, is set in a lower-integer QHE plateau.[11,12] The edge channel of the upper Landau level (LL) ($N = 1$) is reflected at the potential barrier, while the other edge channel of the lowest LL ($N = 0$) is transmitted through the barrier [Fig. 1(b)]. Under such a condition, an edge channel from a source contact collides with one from a drain contact at the diagonal corners of the cross gate [spots B′ and C in Fig. 1(b)]. Our expectation is that photons will be generated at the confluences of edge channels when the difference in electrochemical potential between two adjacent edge channels reaches the LL energy spacing.

II. EXPERIMENTAL SETUP

A scanning THz microscope with single-photon sensitivity has been used to detect extremely weak radiation emitted from edge channels.[13] A quantum-dot (QD) single-THz-photon detector that serves as a single-electron transistor (SET) is incorporated into a scanning confocal optical system [left panel of Fig. 1(c)]. The QD detector is fabricated by standard electron-beam lithography on a GaAs/AlGaAs heterostructure crystal with a 2DEG density $n_{2D} = 3.2 \times 10^{15}$ m^{-2} and a mobility $\mu = 80$ m^2/V s at 4.2 K. The detector is cooled with a ^{3}He refrigerator to $T \simeq 0.3$ K, whereas the measured sample (Hall bar) is maintained at 4.2 K by means of a thermally insulating vacuum layer.

The sample studied is a Hall bar, fabricated by standard photolithography in a GaAs/AlGaAs heterostructure crystal with $n_{2D} = 3.7 \times 10^{15}$ m^{-2} and $\mu = 150$ m^2/V s. Two cross

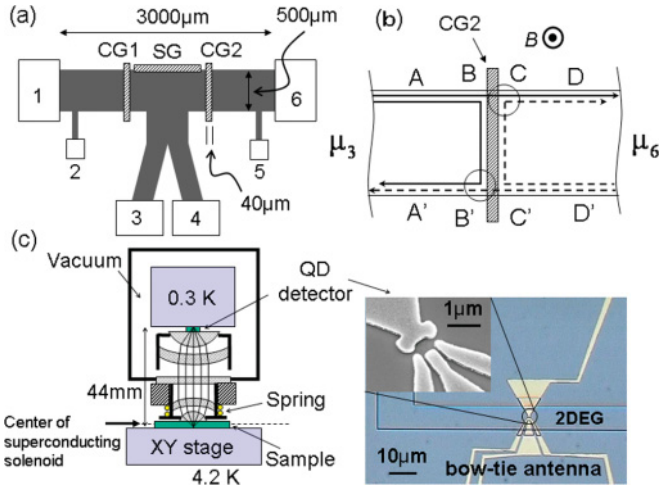

FIG. 1. (Color online) (a) Geometry of the measured Hall bar. (b) Schematic of the Hall bar with a cross gate in the case in which $\nu = 4$ and $\nu_G = 2$. Circles indicate positions at which energy dissipation takes place (spots B′ and C). (c) Schematic of a photon-counting THz microscope (left) and micrograph of the QD detector (right).

gates (CG1 and CG2), each with a length of 40 μm, and a side gate (SG) along the sample boundary are deposited as shown in Fig. 1(a). The side gate is grounded in this study. Data taken by using CG2 and two current contacts (3 and 6) are mainly described in this paper. The electron density, n_{2D}, is tuned by light-emitting diode illumination so that the cyclotron-resonance frequency falls into the detectable range of the QD detector. With a magnetic field of $B = 4.98$ T, the filling factor is set to $\nu = 4.0$ while a negative gate voltage of $V_{CG2} = -0.25$ V results in the region beneath CG2 having $\nu_G = 2.0$. Note that the resonance energy of the QD, $\hbar\omega_{QD} = \hbar\sqrt{(\omega_c/2)^2 + \omega_0^2} + \hbar\omega_c/2$, is slightly larger than the bare cyclotron energy, $\hbar\omega_c$, because of collective plasma oscillations (ω_0 is the plasma frequency of the QD).[14] The resonance energy of the QD is properly matched to the cyclotron energy of the Hall bar (the emitter) when the QD is placed at a distance of 44 mm from the center of the superconducting solenoid [Fig. 1(c)]. The QD is then subjected to a magnetic field of 4.68 T ($\hbar\omega_{QD} = 8.33$ meV) while the Hall bar is in a magnetic field of 4.98 T ($\hbar\omega_c = 8.36$ meV).

III. RESULTS AND DISCUSSION

Photon-counting rates of THz emission around a potential barrier are measured by using the developed THz microscope (Fig. 2). Here, source-drain voltage corresponding to electron energy larger than the LL energy spacing is applied to the emitter (the Hall bar) ($\Delta\mu_{36}/e = V_{63} = 12.9$ mV $> \hbar\omega_c/e$ or a current of $I_{63} = 1$ μA). The dark counting rate is typically about 10 counts per second (cps). The result indicates that THz emission takes place at two confluences of edge channels (spots B′ and C). An edge channel occupied up to μ_3 (or μ_6) is transmitted from a current contact to a corner of the potential barrier and emits THz photons through inter-edge-state scattering with the other occupied up to μ_6

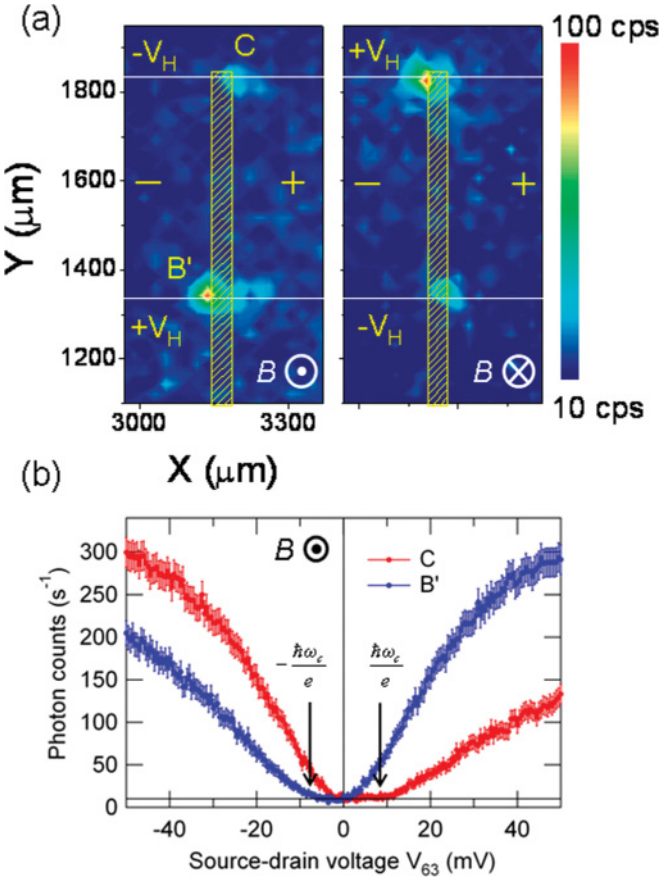

FIG. 2. (Color online) Photon-counting results of THz radiation emitted from edge-channel confluences ($\nu = 4$ and $\nu_G = 2$). (a) Photon-counting images around CG2. (b) Photon-counting rates as a function of the source-drain voltage, $V_{63} = \Delta\mu_{36}/e$, at two confluences (spots B′ and C).

(or μ_3). This photon emission phenomenon is unique in that electrons (or holes) are injected without energy dissipation into a microscopic area where radiation occurs. A feature of the THz imaging results is that the edge-channel confluence at the lower-potential boundary (with positive Hall voltage, $+V_H$) is brighter than that at the higher-potential one; the image acquired under the opposite magnetic-field polarity provides evidence that this is an intrinsic property [Fig. 2(a)]. Broadening of these emission spots in the images is governed by the spatial resolution of our microscope system (~50 μm), and no significant change in the spot size is observed at a larger current of 4 μA. With the extraordinarily high sensitivity of the QD detector, we are able to track to the onset behavior of photon emission [Fig. 2(b)]. At the higher-potential spot (e.g., spot C for positive V_{63}), emission is characterized by an onset voltage corresponding to the LL energy spacing. Beyond our expectation, however, the onset voltage at the lower-potential spot (e.g., spot B′ for positive V_{63}) is substantially lower than the corresponding LL energy spacing.

Figure 3 shows the results for when two potential barriers are introduced across the Hall bar. Here, a current of $I_{16} = 2$ μA is applied between contacts 1 and 6, and the gate voltage, $V_{CG1} = V_{CG2} = -0.25$ V, results in the regions below the gates having $\nu_G = 2.0$. We found six emission spots over the entire

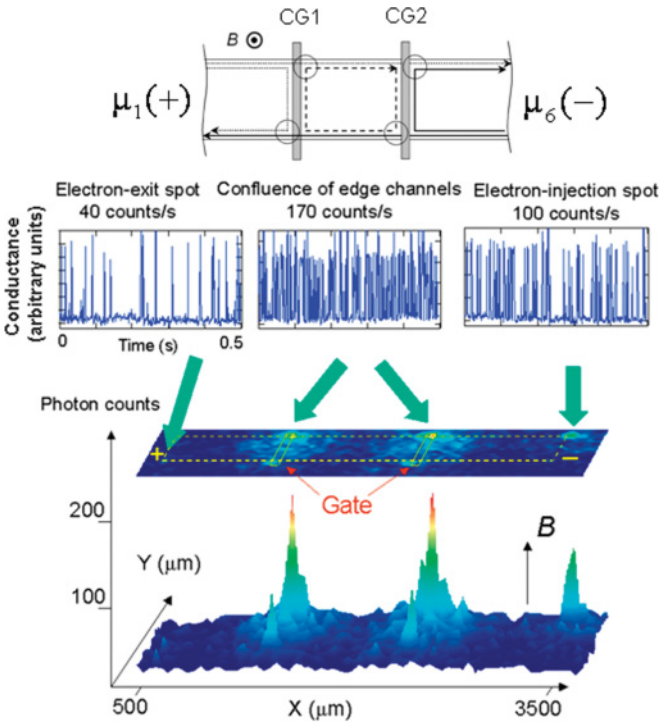

FIG. 3. (Color online) Photon-counting THz imaging of a wide area of the sample. Schematic of the sample structure (top), photon-counting signals at each emission spot (middle), and color mapping of photon-counting rates (bottom).

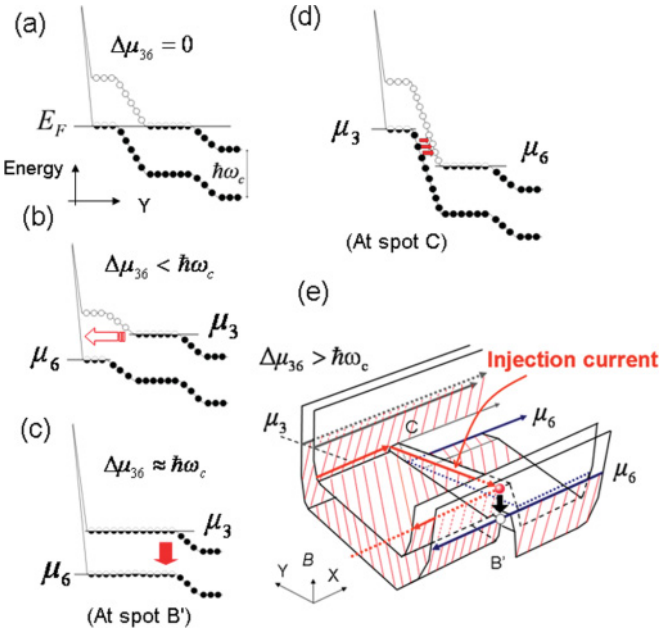

FIG. 4. (Color online) Schematics of edge structures at sufficiently low temperatures. The conditions of the current and the magnetic-field polarity are shown in Fig. 1(b). Energy profiles at spot B′ (a)–(c), spot C (d), and for the whole area of the Hall bar (e).

sample area, namely, electron-injection and -exit spots from current contacts and four edge-channel confluences. Two edge-channel confluences at the lower-potential boundary exhibit the same level of emission intensity and the highest efficiency of all emission spots in the QHE conductor. Apart from being of fundamental interest, this emission phenomenon suggests important aspects for its application: a number of THz point sources can be arrayed via dissipationless channels and the individual sources are gate-controllable.

Let us now consider the mechanism of the optical transition arising from inter-edge-state scattering. First, we address the question of how the edge structure is reconstructed in nonequilibrium conditions. Figure 4 presents a self-consistent energy profile in the edge-channel region at sufficiently low temperatures, as proposed by Chklovskii *et al.*[15] The edge model is applied to nonequilibrium conditions in Ref. 12. The conditions of the current and the magnetic-field polarity are shown in Fig. 1(b). For simplicity, spin splitting is neglected. For $\Delta\mu_{36} < \hbar\omega_c$, the inter-edge-state scattering is determined by tunneling through incompressible strips. At the confluence of edge channels at the lower-potential boundary (spot B′), the electrochemical potential of the outer edge channel is lower than that of the inner edge channel [Fig. 4(b)], resulting in suppression of inter-LL elastic tunneling. When $\Delta\mu_{36}$ reaches $\hbar\omega_c$, the edge structure is reconstructed and inter-edge-state scattering should be strongly promoted via the transition between compressible strips [Fig. 4(c)]. Conversely, tunneling will be promoted at the confluence at the higher-potential boundary [Fig. 4(d)]. The above model of nonequilibrium edge states is supported by transport experiments performed in a quasi-Corbino geometry.[12] Note that electrons emitted from the source contact reach an optically active spot (sport B′) without any scattering. The overview of the energy profile is illustrated in Fig. 4(e), based on a model of self-consistent potential reconstruction under the gate.[16] The emission process found in an earlier work requires the inter-LL tunneling at the higher potential edge and classical drift motion due to the Hall electric field in a dissipative bulk channel.[10] Dissipationless electron injection from the source contact to the optically active spot in a macroscopic device is an appealing feature, allowing us to focus only on suppressing nonradiative processes within the emission spot.

The second question we address is what conditions are necessary for LL emission. The inter-LL optical transition is a vertical $N = 1 \rightarrow 0$ transition; specifically, (i) the $N = 1$ states with wave number k should be occupied by electrons and (ii) the $N = 0$ states with (nearly) the same k should be unoccupied. Since the wave number k determines the center coordinate Y of the position-space wave function through the relation $Y = -l_B^2 k$ in the QHE regime, the above condition implies that electrons should accumulate in the $N = 1$ LL and be depleted in the $N = 0$ LL at a given location within the magnetic length l_B. Therefore, the inter-LL optical transition is allowed at the lower-potential boundary (spot B′) as shown by a thick arrow in Fig. 4(c). Population inversion may be expected if the inter-LL elastic tunneling is sufficiently suppressed.[10] On the other hand, the optical transition is not allowed at the higher-potential boundary (spot C). The excess energy of electrons is mainly released to the lattice system, probably via acoustic phonon emission after inter-LL elastic tunneling [Fig. 4(d)]. This is an intuitive explanation of why the lower-potential spot emits more photons. Indeed, earlier lattice

temperature measurements indicate that the higher-potential spot is more heated than the lower-potential one.[17] However, as shown in Fig. 2(b), the observed onset voltage for photon emission corresponds to less than half of the LL energy spacing. This deviation from LL energy spacing has also been found in transport measurements[12,16] and the origin has not yet been clarified. In addition, there is a theoretical finding that the potential profile underneath the cross gate is self-consistently modified if the source-drain voltage is larger than $\hbar\omega_c/(2e)$.[16] More detailed consideration of the potential profile far from equilibrium will be needed.

Next, let us discuss the possibility of conversion from fermionic electron statistics to photon antibunching in QHE conductors. The necessary conditions for current-induced sub-Poissonian generation are that (i) nonequilibrium carriers are injected by dissipationless conducting channels to an active emission area and (ii) conversion efficiency from injected electrons to photons is sufficiently high. In commercial semiconductor light-emitting devices, injection currents are generated via dissipative bulk transport whereas condition (ii) is properly satisfied ($\eta \geqslant 20\%$). Sub-Poissonian light generation was hence observed when current fluctuations are significantly suppressed by an external high impedance electron source.[1] On another front, condition (i) is mostly fulfilled by edge-channel transport in QHE conductors. Photon conversion efficiency will thus be a critical factor in realizing sub-Poissonian THz generation.

The emission efficiency, $\eta_{\rm emit}$, at 4.2 K is roughly estimated to be on the order of 10^{-4} at spot B′.[18] It follows that most of the excess energy is dissipated through inter-LL elastic tunneling. Considerable suppression of nonradiative tunneling is therefore required for achieving nonclassical photon generation. At lower temperatures below 100 mK, inter-LL tunneling is greatly suppressed[12] but the spin flip-flop process should be considered in the optical transition. Addressing the question of how spin states contribute to LL emission is one of our next targets. Another effective method for reducing the tunneling probability is to introduce a smooth confinement potential by means of a negatively biased gate boundary.

If inter-LL elastic tunneling can be completely suppressed, the equilibration length between adjacent edge channels will be remarkably extended. The probability of the optical transition from the $(N+1)$th to the Nth LL is given by $W_{N+1\to N} = \alpha\sqrt{\epsilon_r}\omega_c^3 l_B^2(N+1)$, where $\alpha = 1.62\times10^{-19}$ s^2 m^{-2} and ϵ_r is the relative dielectric constant.[19] For $\omega_c = 2\pi\times 2.02$ THz and $l_B = 11.5$ nm at $B = 4.98$ T, the transition probability between $N=1$ and 0 is $W_{1\to0} = 1.6\times10^5$ s^{-1}. Since the group velocity of electrons in edge channels is on the order of 10^4 m/s,[16] the equilibration length without nonradiative scattering will reach a scale of ∼0.1 m. This suggests that if photon conversion efficiency is substantially improved, the emission area will be extended over a macroscopic scale along the sample boundary, not limited to the confluence of edge channels.

To get further insight into the emission mechanism, we pushed the potential barrier up higher (i.e., $\nu_G < 2$). As shown in Fig. 5, the emission region progressively evolves upstream along the $N=1$ edge channel injected from the source contact. This feature supports the idea that the upper edge channel plays

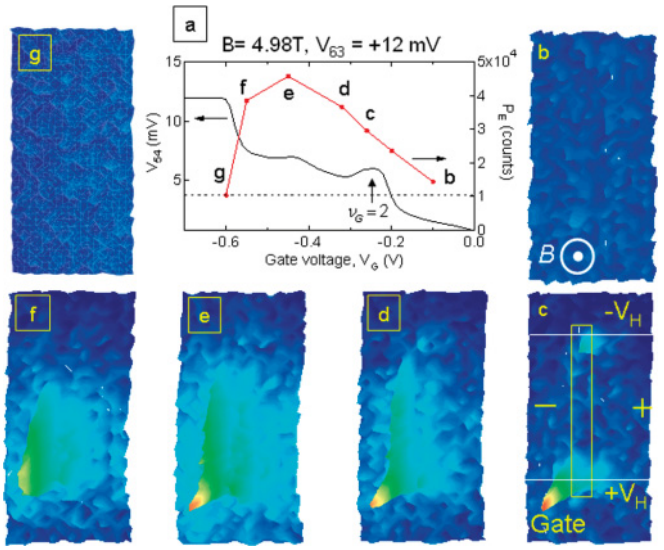

FIG. 5. (Color online) (a) Longitudinal voltages, V_{54}, as a function of the integrated emission intensities, $P_{\rm emit}$. (b)–(g) Photon-counting images for different barrier heights at a source-drain voltage of $V_{63} = 12$ mV.

an important role for electron injection to the emission area. The integrated emission intensity, $P_{\rm emit}$, is enhanced by a factor of 4 at $\nu_G < 2$ despite no significant change in the applied power, V_{63}^2/R_{54} [Fig. 5(a)]. We simply interpret the emission process below. The unoccupied states (holes) in the $N=0$ LL are generated in the gated region at $\nu_G < 2$, whereas the $N=1$ edge channel flows along the gated boundary B-B′. Thereby, charge compensation should be probable between the $N=1$ edge state (electrons) and the $N=0$ unoccupied states (holes) along the boundary B-B′. If the potential profile underneath the cross gate is self-consistently modified and flattened, as suggested in Ref. 16, the charge compensation process will lead to a vertical inter-LL transition rather than the inter-LL elastic tunneling.

IV. CONCLUSION

In conclusion, we have found LL emission at the confluence of edge channels by using a QD photon detector. The edge-channel confluence at the lower-potential boundary emits more photons than that at the higher-potential one. This is because the self-consistent reconstruction of the edge structure allows for a vertical inter-LL transition. Since nonequilibrium electron distributions mediated by noiseless conducting channels and even a level of population inversion are probable, the QHE electron system will be an interesting platform for developing unique THz-photon generators.

ACKNOWLEDGMENTS

We acknowledge financial support from PRESTO of the Japan Science and Technology Corporation (JST) and the Asahi Glass Foundation.

[1]P. R. Tapster, J. G. Rarity, and J. S. Satchell, Europhys. Lett. **4**, 293 (1987); S. Machida, Y. Yamamoto, and Y. Itaya, Phys. Rev. Lett. **58**, 1000 (1987).

[2]C. W. J. Beenakker and H. Schomerus, Phys. Rev. Lett. **86**, 700 (2001).

[3]C. W. J. Beenakker and H. Schomerus, Phys. Rev. Lett. **93**, 096801 (2004).

[4]J. Gabelli, L.-H. Reydellet, G. Fève, J.-M. Berroir, B. Plaçais, P. Roche, and D. C. Glattli, Phys. Rev. Lett. **93**, 056801 (2004).

[5]E. Onac, F. Balestro, L. H. Willems van Beveren, U. Hartmann, Y. V. Nazarov, and L. P. Kouwenhoven, Phys. Rev. Lett. **96**, 176601 (2006).

[6]E. Zakka-Bajjani, J. Segala, F. Portier, P. Roche, D. C. Glattli, A. Cavanna, and Y. Jin, Phys. Rev. Lett. **99**, 236803 (2007).

[7]M. Büttiker, Phys. Rev. Lett. **65**, 2901 (1990).

[8]M. Henny, S. Oberholzer, C. Strunk, T. Heinzel, K. Ensslin, M. Holland, and C. Schönenberger, Science **284**, 296 (1999).

[9]Y. Ji, Y. Chung, D. Sprinzak, M. Heiblum, D. Mahalu, and H. Shtrikman, Nature (London) **422**, 415 (2003).

[10]K. Ikushima, H. Sakuma, S. Komiyama, and K. Hirakawa, Phys. Rev. Lett. **93**, 146804 (2004).

[11]B. J. van Wees, E. M. M. Willems, L. P. Kouwenhoven, C. J. P. M. Harmans, J. G. Williamson, C. T. Foxon, and J. J. Harris, Phys. Rev. B **39**, 8066 (1989); S. Komiyama, H. Hirai, S. Sasa, and S. Hiyamizu, *ibid.* **40**, 12566 (1989); B. W. Alphenaar, P. L. McEuen, R. G. Wheeler, and R. N. Sacks, Phys. Rev. Lett. **64**, 677 (1990); G. Müller, D. Weiss, A. V. Khaetskii, K. von Klitzing, S. Koch, H. Nickel, W. Schlapp, and R. Losch, Phys. Rev. B **45**, 3932 (1992).

[12]A. Würtz, R. Wildfeuer, A. Lorke, E. V. Deviatov, and V. T. Dolgopolov, Phys. Rev. B **65**, 075303 (2002).

[13]K. Ikushima, Y. Yoshimura, T. Hasegawa, S. Komiyama, T. Ueda, and K. Hirakawa, Appl. Phys. Lett. **88**, 152110 (2006).

[14]O. Astafiev, V. Antonov, T. Kutsuwa, and S. Komiyama, Phys. Rev. B **65**, 085315 (2002).

[15]D. B. Chklovskii, B. I. Shklovskii, and L. I. Glazman, Phys. Rev. B **46**, 4026 (1992).

[16]S. Komiyama, H. Hirai, M. Ohsawa, Y. Matsuda, S. Sasa, and T. Fujii, Phys. Rev. B **45**, 11085 (1992).

[17]U. Klaß, W. Dietsche, K. von Klitzing, and K. Ploog, Surf. Sci. **263**, 97 (1992).

[18]The emission efficiency, η_{emit}, is defined as the ratio between the total dissipated power and the radiative power. In order to estimate η_{emit} at spot B′, we refer to an estimated value of $\eta_{\text{emit}} \simeq 10^{-5}$ at the electron-injection spot of the current contact [Y. Kawano and S. Komiyama, Recent Res. Devel. Phys. **3**, 129 (2002)]. First, in our experiments at $I_{63} = 1\mu$A, the photon-counting rate at spot B′ is nearly twice as high as that at the electron-injection spot. Second, the dissipated power localized at spot B′ is calculated to be about one-fourth that at the electron-injection spot.[16] Therefore, the emission efficiency is roughly estimated to be on the order of 10^{-4}.

[19]C. Chaubet, A. Raymond, and D. Dur, Phys. Rev. B **52**, 11178 (1995).